Applications in Engineering Science 26 (2026) 100322

Contents lists available at ScienceDirect

Applications in Engineering Science

journal homepage: www.sciencedirect.com/journal/applications-in-engineering-science

Fatigue behavior of steels for critical members and durability models with stress ratio growth

S. Belodedenko [a], O. Hrechanyi [b,*], M. Scherbinin [a]

[a] Department of Industrial Machinery Engineering, Ukrainian State University of Science and Technologies, Dnipro, Ukraine
[b] Department of Metallurgical Equipment, Zaporizhzhia National University, Zaporizhzhia, Ukraine

ARTICLE INFO

Keywords:
Critical members
High-strength steels
Stress ratio
Fatigue lifetime

ABSTRACT

The use of high-strength steels allows you to reduce the weight of the object, increase reliability and safety. Authors offer a new interpretation of critical members based on risk analysis and the concept of safety. Their performance determines the level of losses during the operation of mechanical systems. Critical members made of high-strength steels can be subjected to cyclic loading with a high stress coefficient. Known disadvantage of high-strength steels is their vulnerability to most impact factors, including cyclic loading with high cycle asymmetry. Cylindrical samples of heat-treated steels 09Cr16Ni4Nb and 13Cr15Ni4NMo3 were tested for tensile fatigue. Test results were presented in the form of a durability equation. Smith charts in relative stresses were obtained by simple transformations from a durability equation. Obtained charts showed a somewhat anomalous concave shape instead of an expected convex. This indicates a loss of sensitivity to mean stresses at high cycle asymmetry. Authors explain this phenomenon from the point of view of combining the concepts of fatigue and fracture mechanics. Model of a durability equation is proposed based on the concept of combining fracture mechanics and fatigue methodology. Its application in practice is a priori and requires assigning only one parameter in the form of the slope of the S-N curve.

Abbreviations

R, stress ratio as index of the asymmetry of load cycle; σ_a, Σm, amplitude and mean cycle stresses; σar, σmr, relative amplitude and mean cycle stresses; σ-1r, relative amplitude stress at r=-1, relative fatigue limit; σr, amplitude of the fatigue limit at stress ratio r; n, number of cycles to the limit state, durability; kσ, stress concentration coefficient; σyk, destruction stress of material in the zones of localization, where kσ>1; m, coefficient of a durability equation, that determine the slope of the s-n curve; br, brr, durability equation coefficients that determine sensitivity to the effects of stress ratio; δσ, stress range, according to which the cyclic value of the sif is determined; δσr, same for relative stresses; γm, γm0 –exponents of the limit amplitude diagram (lad); γ, sensitivity constant of the fatigue threshold to stress ratio; χr, exponent of the critical cyclic toughness model; δkfc0, critical cyclic fracture toughness under σ_m, amplitude and mean cycle stresses; σ_{ar}, σ_{mr}, relative amplitude and mean cycle stresses; σ_{-1r}, relative amplitude stress at R=-1, relative fatigue limit; σ_R, amplitude of the fatigue limit at stress ratio R; N, number of cycles to the limit state, durability; K_σ, stress concentration coefficient; σ_{yk}, destruction stress of material in the zones of localization, where K_σ>1; m, coefficient of a durability equation, that determine the slope of the S-N curve; b_R, b_{RR}, durability equation coefficients that determine sensitivity to the effects of stress ratio; Δσ, stress range, according to which the cyclic value of the SIF is determined; $\Delta\sigma_r$, same for relative stresses; γ_m, γ_{m0} –exponents of the limit amplitude diagram (LAD); γ, sensitivity constant of the fatigue threshold to stress ratio; χ_R, exponent of the critical cyclic toughness model; ΔK_{fc0}, critical cyclic fracture toughness under pulsating loading

1. Introduction

The cycle asymmetry factor was one of the first studied in fatigue methodology. Many models have been developed to take into account its influence. Current surge in research activity into the influence of the cycle asymmetry factor, in the authors' opinion, is due to several reasons. After the sensitivity of fatigue deformation criteria to median stress was discovered, there was a need to verify the invariance of other universal criteria to this factor (Gomes et al., 2025). This is especially true for multiaxial fatigue conditions, where the variety of combinations of individual cyclic processes' action dictates the development of new

* Corresponding author.
E-mail address: hrechanyi@znu.edu.ua (O. Hrechanyi).

https://doi.org/10.1016/j.apples.2026.100322
Received 11 February 2026; Received in revised form 28 March 2026; Accepted 23 April 2026
Available online 23 April 2026

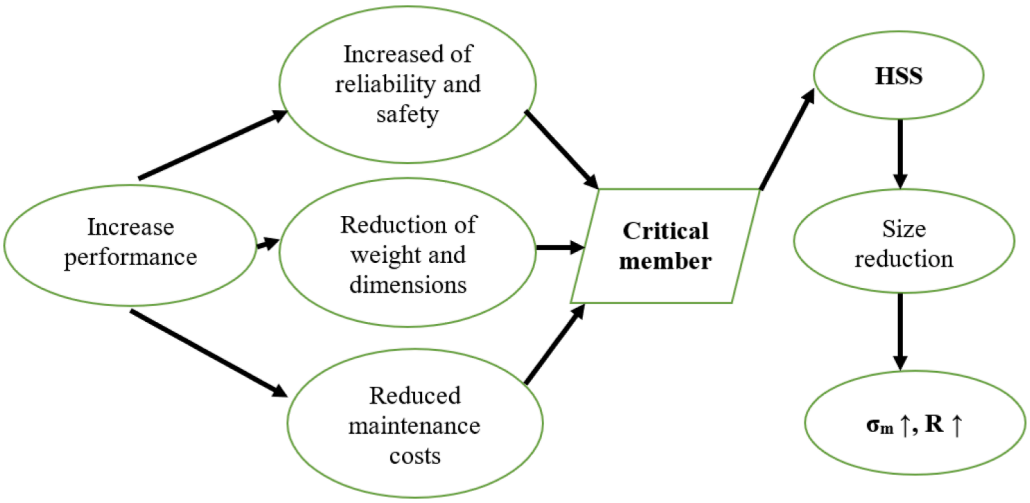

Fig. 1. Solving engineering problems through HSS.

durability models (Gomes et al., 2025; Liu et al., 2024; Abasolo et al., 2024). It is also necessary to take into account the active introduction of composite and additively manufactured parts in mechanical engineering, construction. This also requires checking their behavior under extreme loading conditions, that can include modes with high asymmetry. Also, attention to non-design loading modes with overloads and underloads motivates studying the influence of asymmetry. In fact, the study of modes with underload corresponds to the study of the influence of the cycle asymmetry factor. And finally, increasing the requirements for the safety of structures requires a more accurate assessment of the influence of operational loading, which is characterized by a variation in an average stress.

Another reason for attention to the asymmetry factor may be due to the widespread use of high-strength steels (HSS). They are used to manufacture crucial (important) or critical members of mechanical systems. They are the foundation for solving problems of mechanical science, which are in a state of technical contradiction (Fig. 1). Due to the trend of increasing the functional efficiency of mechanical systems, such requirements are imposed on the latter as increasing reliability and safety along with reducing their weight and dimensions. This contributes to reducing fuel and energy consumption for operation. In addition, the problem of reducing maintenance costs stands out (Krejsa et al., 2025).

Critical members (CM) are made from high-quality materials, which include high-strength steels. CM made of HSS have reduced dimensions and therefore increased overall stress indicators. Such parts and cyclec parts perceive static loads from the weight of the machine (springs), from internal pressure in the shells of units of the metallurgical and chemical industries, from tightening forces (threaded joints), and there are also residual stresses (welded joints). This leads to an increase in the asymmetry of the cycle due to an increase in an average stress. For example, high-strength bolts operate at stress coefficients $R = 0.8$ (Jiao et al., 2025). Interestingly, an asymmetric loading mode is also observed in the shafts of drive mechanisms. Traditionally, it is believed that they operate in a symmetric bending cycle with rotation. But if a low-speed shaft operates in a swinging mode, not making a full rotation during the working cycle, and the load changes, then the symmetric cycle is violated. The authors found that the load shaft of the winch drums maneuvering the cones of the blast furnace loading device suffers from an asymmetric bending at stress coefficients $R = 0.7–0.8$.

Based on the structural and functional analysis, CM are defined by most experts as parts of the machine that perform its main functions. Failure of CM leads to the loss of operability of the object. In addition, the structure of the machine includes auxiliary elements that improve the quality of the main functions of the machine. Their failure may lead to a malfunction of the object, but it will remain operable.

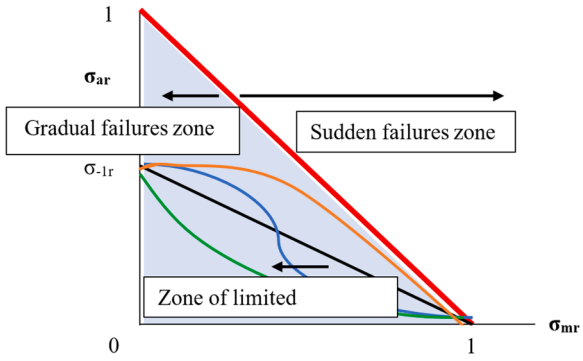

Fig. 2. Using Smith chart to assess reliability and safety.

Based on the risk analysis and the concept of safety, the authors propose a new interpretation of CM. By CM the authors understand parts of machines, the value of which is tens and hundreds of times less than the losses to which their failure leads (Belodedenko et al., 2025). The severity of the failure is used to calculate the criticality level to measure the risk. Special attention is paid to the design and manufacture of such elements. At the operational stage, the forecasting of the resource of CM is carried out mainly using probabilistic-physical models or based on the physics-of-failure. This approach is the basis of the theory of individual structural reliability, which ensures operational safety. As failure analysis shows, not only basic structures and main mechanisms, but also fastening, connection and sealing units can be attributed to CM. They can lead to the initiated failure (Belodedenko et al., 2025; Belodedenko et al., 2020).

The purpose of the paper is to analyze and evaluate the influence of the stress ratio on the durability under uniaxial loading of high-strength steels based on the results of fatigue tests that were conducted in the process of developing a manufacturing technology for critical aerospace parts and members.

2. Theory

The cycle asymmetry factor is characterized by the average cycle stress or by the stress ratio $R = \sigma_{min} / \sigma_{max}$, where the numerator contains the minimum stress and the denominator contains the maximum cycle stress. This is considered, for the most part, with the help of models in the form of Smith or Haigh diagrams. The various existing models are aimed, as a rule, at achieving warranted cyclic strength. Such

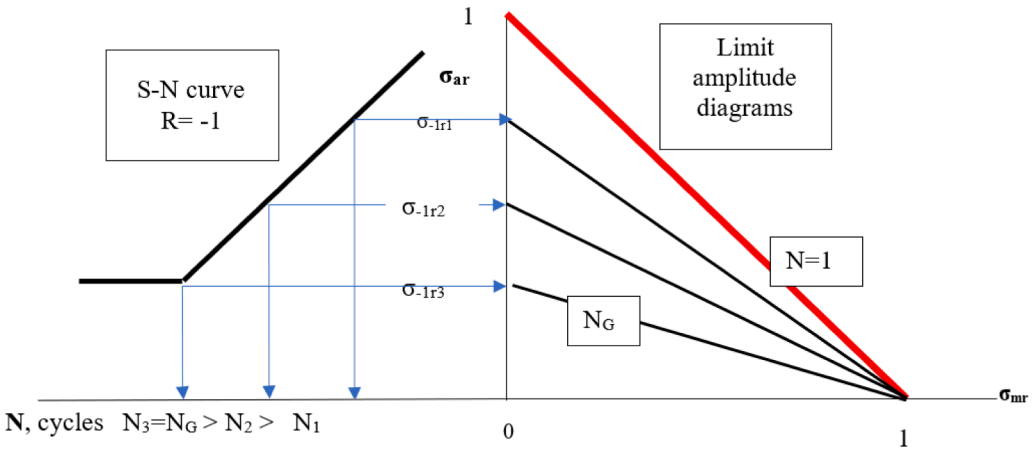

Fig. 3. Effect of bounded durability N on the position of Goodman diagrams.

conservatism is appropriate when designing. However, at the stage of operation, it is worth looking for reserves of durability to help reduce the cost of maintenance and extend the service life of structure.

When using the S-N curves (master curve) as basic fatigue resistance models, it is necessary to reduce the operating cycles of arbitrary asymmetry to the equivalent one, which is usually determined for $R=-1$ or for $\sigma_m=0$. This equivalence is carried out using Smith charts (LAD) that connect the amplitude σ_a and average σ_m stresses of the cycle for a certain endurance N. In Fig. 2, this chart is constructed for the relative values $\sigma_{ar} = \sigma_a/\sigma_u$ and $\sigma_{mr}= \sigma_m/\sigma_u$. The boundary for Smith charts is a straight line connecting points $\sigma_{ar}=1$ and $\sigma_{mr}=1$. Its equation corresponds to the conditions of static failure, when $\sigma_m+ \sigma_a= \sigma_u$. This line separates the zone of sudden and gradual failures. Below the line between the points $\sigma_{ar}= \sigma_{-1r}$ and $\sigma_{mr}=1$ is the zone of limited endurance. The shape of this line can be varied, based on the equation of LAD. Actually, finding out the shape of LAD is the purpose of studying the influence of cycle asymmetry on durability. Below the LAD line is the non-destructive zone up to durability N.

The most common form of LAD, which connects points σ_{-1r} and $\sigma_{mr}=1$, is the linear or the Goodman model (Fig. 3). Sometimes the line, which connects points σ_{-1r} and $\sigma_{mr}=1$, is described by using a piecewise function. Their tilt characterizes the sensitivity of the material to cycle asymmetry. The smaller it is, the smaller the tilt to the horizontal axis of the LAD segment. In addition, there are LADs of convex, concave and mixed convex-concave shapes (Fig. 2).

Almost all forms of LAD are satisfied by the equation

$$\sigma_{ar} = \sigma_{-1r}\cdot[1 - (\sigma_{mr})^r]^\alpha, \quad (1)$$

where r and α – equation parameters.

If $r=\alpha=1$, then we obtain the linear Goodman model. In this case, the reduction in cyclic strength or ultimate amplitude is proportional to the reduction in static strength due to the average stress. Depending on the combination of parameters r and α, LAD can have a convex or concave shape. Recently researchers have proposed LAD equations containing trigonometric functions (Krizhanovsky et al., 2008). Such models can take into account convex and concave sections in one LAD at N = const.

Practice shows that in a wide range of durability, asymmetry of cycles and material properties, LAD have a convex shape and their concave shape is rather perceived as an anomaly. For example, testing of titanium alloy samples at R = 0.5–0.7 showed a sharp drop in fatigue strength in the region of low stress amplitude. In this case LAD obeys the Gerber dependence, which gives a convex shape (Belodedenko et al., 2024; Karolczuk and Kurek, 2025). Despite the variety of LAD shapes, in the canonical interpretation they all must intersect the points σ−1r and σmr=1. The latter point coincides with the LAD limit and corresponds to the principles of continuum mechanics.

LAD position is influenced by factors of the ultimate endurance N the most, for which the diagram is constructed, as well as the stress concentration K_σ. The principle of their action is explained for linear Goodman diagrams (Figs. 3 and 4). As can be seen, the boundary of the Smith chart can be perceived as LAD for N = 1 and K_σ=1. The lowest position is occupied by LAD for unlimited durability N_G. For a smaller number of cycles LAD have a more convex shape. The increase in each factor leads to a decrease in the sensitivity of ψ_R and the shape of LAD goes from convex to concave. This is due to the fact that the effective

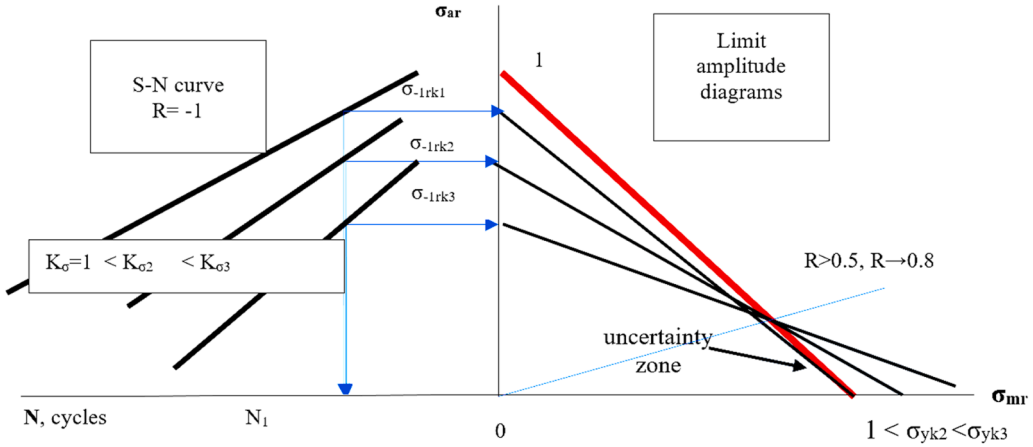

Fig. 4. Effect of stress concentration factor K_σ on the position of Goodman diagrams.

Table 1
Chemical composition of the studied steels, weight- %.

Steel	Chemical elements								
	C	Mn	Si	Cr	Ni	Nb	S	P	Mb
09Cr16Ni4Nb	0.1	0.4	0.5	16	4	0.15	0.015	0.02	-
13Cr15Ni4NMo3	0.12	0.45	0.46	15.1	4.37	-	0.01	0.027	2.48

Table 2
Mechanical properties of the studied steels.

Steel	Indicators of properties				
	Tensile strength, σ_v, MPa	Yield strength $\sigma_{0.2}$, MPa	Reduction of area, %	Elongation, %	Hardness, HRc
09Cr16Ni4Nb	1147	935	53	-	-
13Cr15Ni4NMo3	1552	1373	52	16	42

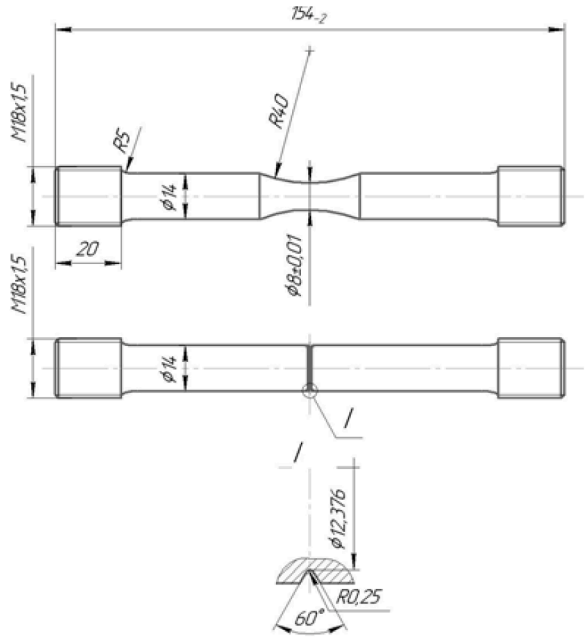

Fig. 5. 13Cr15Ni4NMo3 steel sample drawings.

concentration coefficient for average cycle stresses is much lower than the similar characteristic for amplitude stresses. At the same time, the zone of limited durability narrows, and hence the range of safe loading modes narrows. This is also facilitated by an increase in the stress coefficient R.

In the zone of high asymmetries, safe operation is possible only for small amplitudes. An unusual situation is created when the material undergoes elastoplastic deformations that are characteristic for low-cycle fatigue, and the durability corresponds to the region of multi-cycle fatigue. The behavior of the material in such conditions is not certain (uncertainty zone, Fig. 4). Sometimes such conditions are modeled as a combination of damage from low-cycle and multi-cycle fatigue (Yue et al., 2024). The increase in the static strength of the material under the conditions of localization σ_{yk} gives grounds to the existence of LAD outside the line from σ_{ar}=1 to σ_{mr}=1. The same effect is observed in the presence of cracks. This cannot be explained in terms of classical mechanics.

There was a need to study the fatigue resistance of HSS with significant positive cycle asymmetry in more detail, when the stress ratio is R = 0.5…0.8.

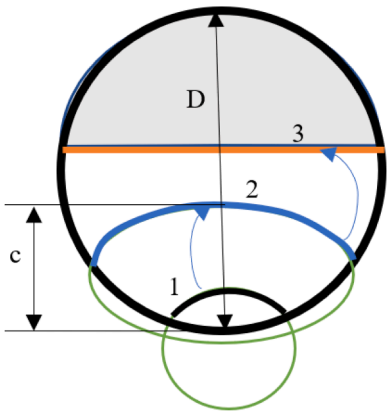

Fig. 6. Diagram of the evolution of the crack front's shape during its propagation under the action of cyclic stretching: from semicircle 1, to semiellipse 2 and segment 3.

3. Materials and methods

Fatigue tests were performed on samples of two steels (Tables 1 and 2). They are used in aerospace engineering for the manufacture of CM. In particular, steel 13Cr15Ni4NMo3 is used for the manufacture of bolts for fastening aircraft wheels. Steel 09Cr16Ni4Nb is used in missile systems.

According to all classifications both steels can be classified as HSS. The heat treatment of the samples corresponded to the heat treatment of steels, which is specified in the drawings of the parts. The blank for the samples of steel 13Cr15Ni4NMo3 of electroslag remelting was a hot-rolled bar with a diameter of 22 mm (Fig. 5). Unnotched (smooth) samples were hourglass shaped, 8 mm in diameter and stress concentration factor K_σ=1. The groove of the notched samples imitated the recess of a metric thread with a pitch of 1.5 mm. It was applied after heat treatment and for such samples K_σ=4 was adopted.

Bolts with a knurled thread M18 and a pitch of 1.5 mm were also made from 13Cr15Ni4NMo3 steel (Belodedenko et al., 2020). Their test modes corresponded to the test modes of the samples (Belodedenko et al., 2023). When analyzing these results, only those that were destroyed in the thread were taken into account.

Samples from 09Cr16Ni4Nb steel were made uncut, similar in shape to the samples in Fig. 5. However, for them the working part had a diameter of 9 mm, and the gripping heads were made with a M24 thread. The workpiece in this case was a bar with a diameter of 80 mm. The working surface of the samples was formed after heat treatment by grinding, its roughness did not exceed the arithmetic mean deviation of the profile of 0.63 μm.

Tests under stationary axial load were carried out at a frequency of 5–15 Hz. For alternating test modes at $-1 < R < 0$, a servo-hydraulic

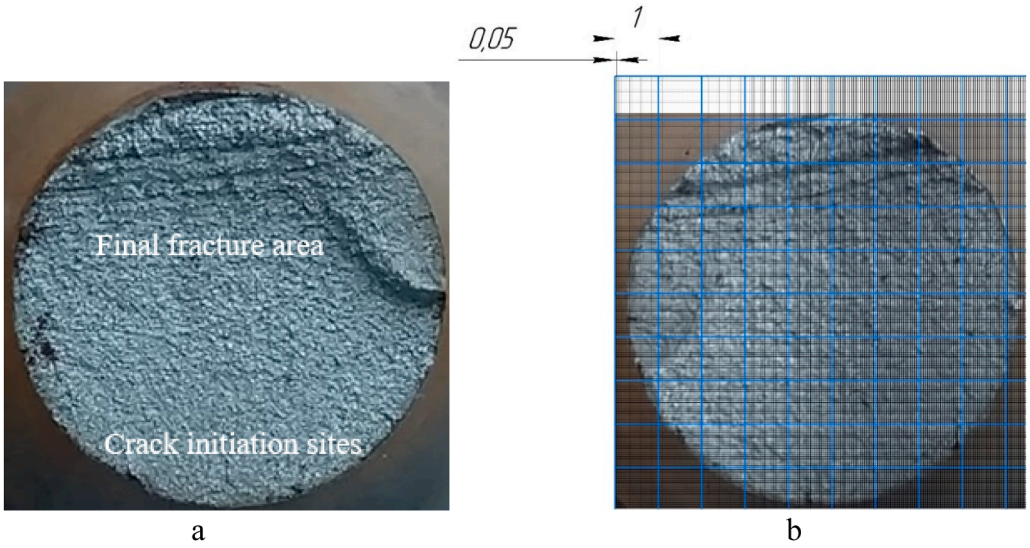

Fig. 7. Typical macro-morphology of the unnotched samples: a – evolution of the crack; b - measuring crack's size using a measuring grid.

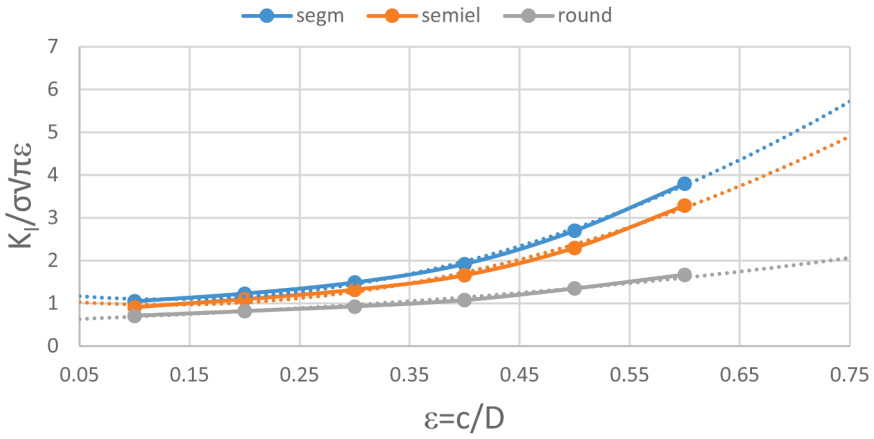

Fig. 8. Geometric factors for edge cracks of round, semi-elliptical and segmental shape in a round rod under tensile strength (Carpinteri's solution).

Table 3
Modes and results of fatigue tests *lgNe* of steel 09Cr16Ni4Nb samples, as well as their comparison with the calculated *lgN* according to the models (2).

Experiment No.	$R > 0$					$-1 \le R \le 0$				
	$lg\Delta\sigma$, MPa	R	$lgNe$	Sl_{gNe}	lgN	$lg\Delta\sigma$, MPa	R	$lgNe$	Sl_{gNe}	lgN
1	2.87	0.6	3.44*	0.07	3.46	3.18	0	2.60*	0.05	2.60
2	2.87	0.2	4.87	0.137	4.78	3.18	−1	4.09	0.101	4.10
3	2.64	0.6	5.30	0.157	5.28	3.00	0	4.10	0.101	4.12
4	2.64	0.2	6.60	0.217	6.60	3.00	−1	5.90	0.184	5.94
5	2.87	0.4	4.15*	0.104	4.18	3.18	−0.5	3.79*	0.087	3.80
6	2.64	0.4	6.03	0.190	6.00	3.00	−0.5	5.00	0.143	5.04
7	2.76	0.6	4.37*	0.114	4.37	3.09	0	3.35*	0.067	3.35
8	2.76	0.2	5.60	0.171	5.70	3.09	−1	5.00	0.143	5.07
9	2.76	0.4	5.10	0.148	5.09	3.09	−0.5	4.45	0.118	4.41

*- the result is corrected by extrapolation, since the mode is not possible

type testing machine was used. For constant test modes at $R > 0$, a hydraulic type testing machine with a pulsator was used. Tests were carried out until the samples were completely destroyed, when the durability N was determined.

After the tests the fractures of the samples were analyzed measuring the final fracture area (Figs. 6, 7). Shape of the crack front, which affects the geometric factor in determining the stress intensity factor (SIF), changed depending on the value of N. The most common way of changing the crack front: 1 semicircle → 2 semiellipse → 3 segment (Fig. 6). Although this is not a dogma. There were cases when the critical relative crack depth ε=c/D →0.75, and the shape remained semicircular. There were also opposite cases. Macroscopic morphological features of the fracture surfaces for selected samples are presented in Fig. 7.

After determining the critical crack size ε_c, the critical cyclic toughness ΔK_{fc} was determined for fracture mode I. For this purpose previously obtained dependences for round rods were used, which were approximated under the research conditions (Fig. 8) (Toribio et al.,

Table 4
Modes and results of fatigue tests *lgNe* of 13Cr15Ni4NMo3 steel samples, as well as their comparison with the calculated *lgN* according to the models (2).

Experiment No.	K_σ=1					K_σ=4				
	$\Delta\sigma$, MPA	R	$lgNe$	S_{lgNe}	lgN	$\Delta\sigma$, MPA	R	$lgNe$	Sl_{gNe}	lgN
1	867	0.627	4.54*	0130	4.48	290	0.627	4.77	0.061	4.75
2	867	0.100	4.76	0.132	4.78	290	0.100	5.04	0.076	5.03
3	537	0.627	5.75	0.178	5.77	232	0.627	5.23	0.086	5.23
4	537	0.100	6.08	0.194	6.07	232	0.100	5.50	0.101	5.51
5	867	0.363	4.48	0.127	4.50	290	0.363	4.84	0.064	4.80
6	537	0.363	5.82	0.182	5.79	232	0.363	5.35	0.093	5.37
7	682	0.627	5.08	0.147	5.13	260	0.627	5.01	0.074	4.99
8	682	0.100	5.41	0.163	5.42	260	0.100	5.31	0.091	5.27
9	682	0.363	5.12	0.149	5.14	260	0.363	5.15	0.082	5.13

* - the result is corrected by extrapolation, since the mode is not possible.

Table 5
Values of a durability Eq. (3) coefficients for absolute (MPa, numerator) and relative (denominator) stress when amplitude is doubled $\Delta\sigma$, $\Delta\sigma_r$.

Object No.	Object type	Range	b_o/b_{0r}	M	b_R	b_{RR}	b_{mR}
1a	Steel 09Cr16Ni4Nb, K_σ=1	$R > 0$	28.3 / 3.67	8.05	2.04	−1.58	0
1	Steel 09Cr16Ni4Nb, K_σ=1	$-1 \le R \le 1$	31.5 / 3.71	9.07	0.51 / 2.77	−1.70	−0.74
2	Steel 13Cr15Ni4NMo3, K_σ=1	$R > 0$	23.2 / 3.37	6.20	1.92	1.87	0
3	Steel 13Cr15Ni4NMo3, K_σ=4	$R > 0$	17.3 / 1.47	4.96	0.53	0	0
4	Steel 13Cr15Ni4NMo3, bolt M18	$R > 0$	40.3 / −1.88	13.2	2.54	0	0

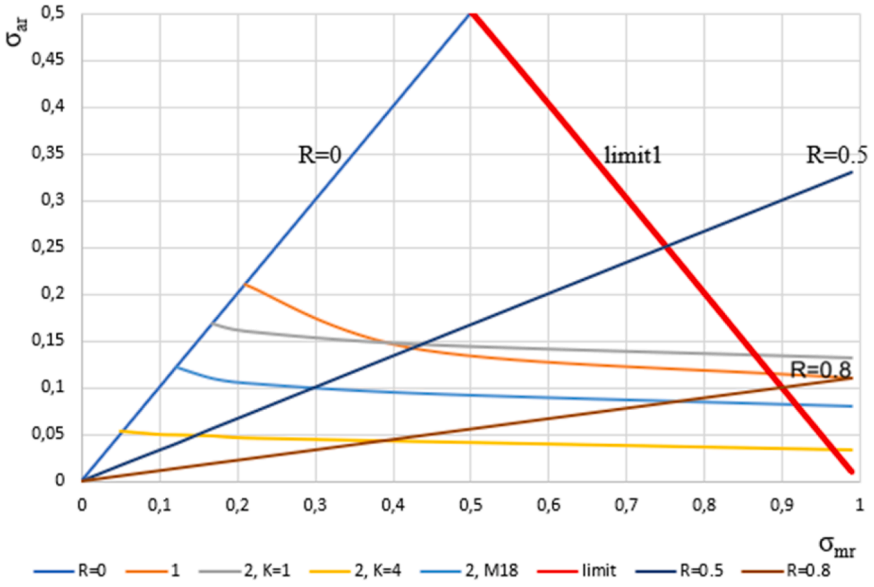

Fig. 9. Comparative LAD of the 09Cr16Ni4Nb steel when K_σ=1 (1), 13Cr15Ni4Mo3 steel when K_σ=1 (2), when K_σ=4 (2, K=4), M18 bolts made of this steel with knurled thread (M18) in the asymmetrical positive cycle.

2022; Toribio, 2022; Carpinteri, 1992).

At the first stage, unnotched samples of 09Cr16Ni4Nb steel were tested in a wide range of changes in the asymmetry of the R cycle, i.e. in tension-compression. The test conditions were designed so that the multiple regression equation could be obtained (Table 3):

$$\lg N = b_0 - m\cdot\lg\Delta\sigma - b_R\cdot R + b_{RR}\cdot R^2, \quad (2)$$

where b_0, m, b_R, b_{RR} – model coefficients that determine the sensitivity of durability to the influence of a certain factor; $\Delta\sigma=2\sigma_a$ – double amplitude of the cycle stresses.

This model is called a durability equation, from which both S-N curves and Smith charts can be obtained (Belodedenko et al., 2020). In this case, a durability equation takes the meaning of the master model instead of the common master S-N curve.

In the second stage, notched samples were tested in the positive asymmetry zone of the R cycle, i.e., under cyclic stretching (Table 4).

A durability equation also has an expression for relative stresses $\Delta\sigma_r = 2\sigma_a/\sigma_y$ (Table 5):

$$\lg N = b_{0r} - m\cdot\lg\Delta\sigma_r - b_R\cdot R + b_{RR}\cdot R^2. \quad (3)$$

At each point of the plan or the experiment (Tables 3, 4), 3–5 samples were tested. The accuracy of the results can be judged by the standard deviations of the logarithms of the durability S_{lgNe}. The error between the experimental results of *lgNe* and the calculations using the *lgN*

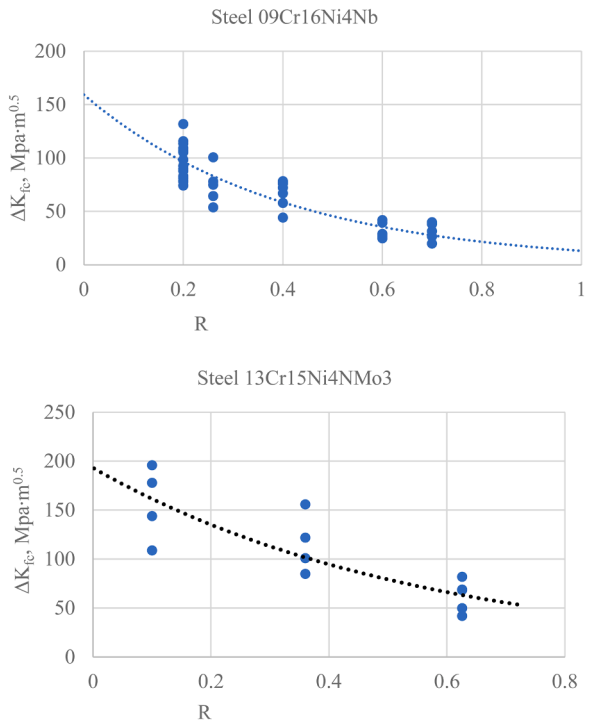

Fig. 10. Experimental models of the relationship between the cyclic fracture toughness and the cycle asymmetry of steels.

models (Tables 4, 5) does not exceed 10 %, which may indicate the adequacy of models (2) and (3).

LAD obtained from a durability equation have a concave shape and can be approximated by an exponential equation over a wide range of cycle asymmetry (Fig. 9):

$$\sigma_{ar} = \sigma_{-1r}\exp(-\gamma_m\sigma_{mr}), \tag{4}$$

$$\sigma_{ar} = \sigma_{0r}\exp(-\gamma_{m0}\sigma_{mr}), \tag{5}$$

where σ_{-1r} and σ_{0r} – respectively, fatigue limits in symmetric and pulsating modes; γ_m, γ_{m0} – LAD parameters. For the studied objects, the parameter γ_{m0} was changed from 0.27 to 0.70.

In the zone of high cycle asymmetry ($R > 0.5$) obtained LAD can be approximated by linear equations:

$$\sigma_{ar} = \sigma_{0r} - \gamma_R R, \tag{6}$$

where – γ_R – LAD parameter.

The dependence of the critical cyclic fracture toughness ΔK_{fc} on the value of R can be approximated by an exponential dependence (Fig. 10):

$$\Delta K_{fc} = \Delta K_{fc0}\exp(-\chi_R R), \tag{7}$$

where ΔK_{fc0} – critical cyclic fracture toughness in pulsating mode; χ_R – model's parameter. For the studied steels, this parameter is 2.42 (Steel 09Cr16Ni4Nb) and 1.88 (Steel 13Cr15Ni4NMo3). At the same time, the average destruction rates are ΔK_{fc0}=151 MPa•m$^{1/2}$ (Steel 09Cr16Ni4Nb), ΔK_{fc0}=198 MPa•m$^{1/2}$ (Steel 13Cr15Ni4NMo3). The coefficient of variation of the ΔK_{fc} indicator at one fixed level R=*const* is ν_{Kfc}=0.12–0.15, which is approximately twice as high as is usually observed in standard tests. Fracture toughness was determined on round samples for fatigue tests. There were 3 types of the critical crack front's shape (Fig. 6). The crack did not always «have time» to acquire a segmental shape. This introduced a certain uncertainty into the choice of the working dependence for the geometric factor (Fig. 8). Nevertheless, the $\Delta K_{fc}(R)$ models of the exponential form (7) have the highest index of the closeness of the correlation relationship, denoted as Cor^2. For Steel 09Cr16Ni4Nb Cor^2=*0.80*, for Steel 13Cr15Ni4NMo3 Cor^2=*0.85* (Fig. 10).

4. Results and discussion

Two models of the exponential type were obtained for LAD in a wide range of stress ratio R. One master *S-N*-curve found at values $R = -1$ or $R = 0$ is enough to construct for the models. For $R = 0$ the correlation between the cycle parameters is higher. For $R > 0$ the model of LAD analogues has been obtained, which has a linear shape. Analogues of LAD are built in the coordinates of the amplitude stress σ_a – stress ratio R. The authors explain researched phenomena from the standpoint of the merging of fatigue and fracture mechanics concept (MFFM-concept).

4.1. Directions of the merging of fatigue and fracture mechanics concept

The main connections between the two theories were formulated in 1998 by Newman (Newman, 1998). First, this is the analysis of local stresses in the vicinity of the crack tip. It is used to calculate the SIF. Second, the fatigue life is presented as the period of growth of short cracks. Later, the method of survival curves developed from this direction, which determines the number of crack growth cycles to the critical size. Third, taking into account the phenomenon of crack closure/opening to predict durability in the unsteady regime. Newman considers the development of the theory of short cracks to be the main achievement of the MFFM-concept.

Another direction is taken from the MFFM-concept. A well-established model to predict the fatigue limit in the presence of small, crack-like defects is the so called $\sqrt{}$area-parameter model proposed by Murakami and Endo (More et al., 2025). Critical flaw size, $\sqrt{area\ critical}$, is the maximum size before defects become non-detrimental. Kitagawa-Takahashi diagram for crack-like defect (σ_{-1} vs. $\sqrt{area}$). The 3 times increase in defect size of magnitude from 1 μm 1000 μm can lower the endurance limit by 300 MPa.

Safe size of crack-like and notch-like defects are also determined by the Frost diagram (σ_{-1} vs. K_σ) and the Nisitani diagram (σ_{-1} vs. $1/\rho$). Critical size of the $\sqrt{area_c}$ and notch-root radius ρ_c are fundamental constants of the material. With their help, it is possible to determine the endurance limits and other parameters of the S-N curve (More et al., 2025). In simpler cases, material with cracks can be characterized by its critical length a_c (Lukáš and Kunz, 1981; Lukash and Kunz, 1983). Its value depends on the material and does not depend on the loading regime and method. The stronger the material, the smaller the value a_c. In the studied metals the crack length a_c, which corresponds to the transition from diffuse fatigue damage to the stage of crack growth, is hundredths of a millimeter. The size a_c is tenths of a millimeter in steels of normal strength. Along with the critical defect sizes, the material has a threshold SIF ΔK_{th}. If the current ΔK is less than the threshold, the crack does not propagate. Both of these fundamental indicators form the endurance limit σ_{-1}. Cracks may appear at such stress, but they do not lead to failure. Therefore, the estimation of the parameters of fatigue resistance models based on short crack models is a relevant task.

But in the early stages of the development of fracture mechanics, the Paris model of crack growth was difficult to obtain, since its parameters are interdependent and sensitive to the metal structure (Kujawski and Ellyin, 1984). Therefore, the inverse problem was solved: finding the crack growth rate using low-cycle fatigue models for the transformation zone behind the crack tip. To do this, deformation or energy fatigue criteria are substituted into the Paris equation instead of its constant. The accumulation of damage in the plastic zone occurs proportionally to the growth of the fatigue crack.

One of the displays of the MFFM concept is the theory of critical distances (TCD), which estimates durability based on stresses determined at certain distances from the root of the notch, or averaged over areas or volumes around the critical notch (Li et al., 2025; Taylor, 1999; Susmel, 2013). It is believed that a crack can grow if it is formed at a

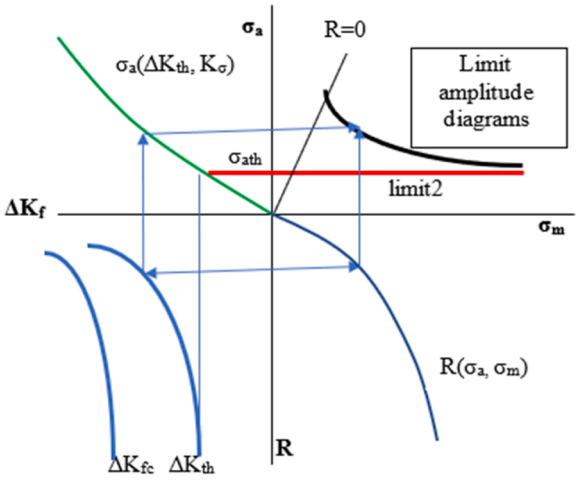

Fig. 11. Diagram of formation of LAD for unlimited endurance N_G according to the threshold SIF ΔK_{th}.

critical distance (CD) from the root of the notch. Cracks located closer to the root are short and do not develop. If local stress at the CD from the crack tip exceeds the fatigue limit of the smooth sample, the crack will propagate, ultimately leading to fatigue failure. CD is determined by the threshold of stress intensity factor range and the fatigue limit, while the two parameters must be determined under the same stress ratio. Both indicators characterize both fracture mechanics and fatigue theory.

The result of the development of the MFFM concept can be considered as the processes of fatigue damage accumulation and fracture development are explained by phenomena at the microlevel. In terms of current research on the influence of cycle asymmetry, the theory of crystal plasticity (CP) is valuable. This theory offers an effective basis for solving these problems, allowing to model deformation at the grain level and fix the micromechanisms that control the occurrence of fatigue cracks (He et al., 2025; Jiao et al., 2025). From the standpoint of CP, the mechanism of ratcheting is explained, that is, the process of directional accumulation of plastic deformations during cycling (Zhao et al., 2025). The mechanism of ratcheting at the microlevel explains the effect of the average stress or stress coefficient, both on the fatigue limit and on the cyclic fracture toughness (Shiozawa et al., 1998; Zeng et al., 2025). Integration with modern methods of fracture mechanics is significantly manifested in the study of the topography of fracture surfaces (Macek et al., 2021). This is a rather powerful way to establish the true causes of fracture, especially important in multiaxial fatigue.

4.2. Durability equation model based on threshold SIF

The loss of sensitivity to cycle asymmetry for high-strength steels can be explained by a similar phenomenon for the parameters of the Paris diagrams. With an increase in cycle asymmetry after a certain R, the values of the threshold ΔK_{th} and critical ΔK_{fc} cease to decrease (Fig. 10). Moreover, the range of ΔK_{fc} change is less than the range of ΔK_{th}. This feature is associated with the phenomenon of crack closure and the appearance of oxides on its banks (Anon, 1990).

Relationship between the values of ΔK_{th} and the amplitude of the endurance limit σ_a is carried out through the σ_a (ΔK_{th}, K_σ) function, the form of which depends on the loading method, the level of stress concentration or the sharpness of the notch (Fig. 11). Therefore, this relationship can have a different form (Lukáš and Kunz, 1981). As can be seen from the LAD formation diagram (Fig. 11), the forms of the functions $\Delta K_{fc}(R)$, $\Delta K_{th}(R)$, $\sigma_a(\sigma_m)$ are similar to each other.

The concave nature of LAD is explained by the existence of some minimum possible endurance limit σ_{ath}, which corresponds to the value of ΔK_{th}. Therefore, LAD line cannot reach the point $\sigma_m=\sigma_{yk}$ or $\sigma_{mr}=1$. In fact, the limit of existence of LAD from the straight line between the points $\sigma_{ar}=1$ to $\sigma_{mr}=1$ (limit 1, Fig. 10) crosses into the limit $\sigma_a=\sigma_{ath}$ (limit 2, Fig. 11). Below this line, the mechanism of material failure changes. The material can enter the zone of so-called static fatigue with failure from plasticity exhaustion. There a transition from creep-fatigue to creep-ratcheting emerges (Bai et al., 2025). Or the material fails from an internal crack in the zone of very high-cycle fatigue. For example, for titanium alloy samples at $R > 0.5$, fatigue failure began from a subsurface crack (Shiozawa et al., 1998). According to the authors, the first case is typical for materials that undergo cyclic softening. The second case is typical for materials that undergo cyclic hardening.

Assuming that the value of a_c is a material constant, a power-law model of the threshold SIF ΔK_{th} (R) is proposed (Lukash and Kunz, 1983; Lukáš and Kunz, 1981). Hence, the amplitude of the fatigue limit under asymmetric loading σ_R is determined by a similar dependence:

$$\sigma_R = \sigma_{-1}\cdot\left(\frac{\sigma_{\max}}{\sigma_a}\right)^{-\gamma}, \tag{8}$$

where γ=0…1 – material constant characterizing the sensitivity of threshold values to cycle asymmetry; σ_{max} – maximum operating cycle stress.

Using the value R to characterize the asymmetry, we obtain

$$\sigma_R = 2^{-\gamma}\cdot\sigma_{-1}\cdot(1-R)^{\gamma}. \tag{9}$$

The last two equations represent LAD. Their graphs have a concave appearance. The well-known hyperbolic Oding equation corresponds most closely to such forms of LAD (Oding, 1962): $\sigma_R^2 + \sigma_R\cdot\sigma_m = \sigma_{-1}^2$.

The disadvantage of this dependence is associated with a fixed ratio of amplitudes for symmetric (R=−1) σ_{-1} and pulsating ($R = 0$) σ_0 cycles: $\sigma_{-1}=\sigma_0\sqrt{2}$. This is not always done.

The Oding equation can be represented in terms of the quantity R:

$$\sigma_R = 2^{-0.5}\cdot\sigma_{-1}\cdot(1-R)^{0.5} = \sigma_0\cdot(1-R)^{0.5}. \tag{10}$$

When γ=0.5 Eqs. (8) and (10) are identical. For the considered range of asymmetries, the fatigue limits determined by these equations with a tolerance of 10 % correspond to a durability Eq. (2) (Table 7).

Thus, dependencies (8) and (9) are a theoretical confirmation of the experimental model (2). Expressing the amplitude σ_0 at $R = 0$ from the equation of the S-N curve, after logarithmization, we finally obtain:

$$\lg N = b_0 - m\cdot\lg\sigma_R + 0.5\cdot m\cdot\lg(1-R). \tag{11}$$

Structurally, this dependence corresponds to a durability equation and allows avoiding the experimental determination of the coefficients e_R and e_{RR}.

4.3. Recommendations for applying the results

The recommendations from the FKM-guideline “Analytical strength Assessment” support the use of concave LAD models. It proposes the Haibach model, where the LAD consists of 4 sections of piecewise linear functions (Rennert et al., 2024; Haibach, 2006). The slope in the last sections in the sign-invariant region of the regimes ($R > 0$) is three times smaller than the slope of the LAD for sign-changing regimes ($\sigma_m < 0$). A decrease in the slope is proportional to the decrease in sensitivity to cycle asymmetry.

Since the studied materials are usually used in the manufacture of critical parts, it is advisable to obtain LAD for them directly by fatigue tests in the form of a durability Eq. (2). Here, the asymmetry of the cycle is estimated by its coefficient R, and not by the value of σ_m, for which the coefficient of the model of type (2) is very small. The traditional LAD $\sigma_a=f(\sigma_m)$ agrees better with fatigue curves in semi-logarithmic coordinates. The proposed model corresponds to modern ideas about fatigue curves in double logarithmic coordinates. It is also devoid of the main drawback of theoretical LAD, where the durability value N affects their shape. When reducing asymmetric cycles to equivalent symmetric ones, this leads to inaccurate calculation of parts for limited durability.

Table 6
Model parameters for estimating the effect of the cycle asymmetry based on $N = 2000{,}000$ cycles.

Object No.	Object Type	Model No.							
		(4)		(5)		(6)		(7)	
		σ_{-1r}	γ_m	σ_{0r}	γ_{m0}	σ_{0r}	γ_R	ΔK_{fc0}, MPa•m$^{1/2}$	χ_R
1	Steel 09Cr16Ni4Nb, K_σ=1	0.33	1.13	0.21	0.70	0.20	0.125	151	2.42
2	Steel 13Cr15Ni4NMo3, K_σ=1	0.18	0.33	0.17	0.27	0.17	0.05	198	1.88
3	Steel 13Cr15Ni4NMo3, K_σ=4	0.06	1.02	0.05	0.39	0.05	0.01	-	-
4	Steel 13Cr15Ni4NMo3, bolt M18	0.12	0.45	0.12	0.50	0.12	0.05	-	-

Table 7
Comparison of the relative amplitudes of the fatigue limits σar based on $N = 2000{,}000$ cycles obtained experimentally (numerator) and according to the model of the threshold SIF (5.4) (denominator).

Object No.	Object Type	R			
		−1	0	0.4	0.8
1	Steel 09Cr16Ni4Nb, K_σ=1	0.33 0.37	0.26 0.26	0.19 0.20	0.12 0.12
2	Steel 13Cr15Ni4NMo3, K_σ=1	0.22 0.20	0.17 0.17	0.15 0.137	0.13 0.119
3	Steel 13Cr15Ni4NMo3, K_σ=4	0.07 0.06	0.053 0.053	0.048 0.045	0.044 0.040
4	Steel 13Cr15Ni4NMo3, bolt M18	-	0.122 0.122	0.100 0.092	0.086 0.08

For example, the use of the most widely used Goodman model in comparison with the obtained models underestimates the equivalent stresses for the pulsating cycle $R = 0$ from 12 % (Steel 09Cr16Ni4Nb, K_σ=1) to 48 % (Steel 13Cr15Ni4NMo3, K_σ=4). This difference is amplified with increasing asymmetry: for $R = 0.75$, the Goodman model underestimates the equivalent stresses by 50 % (Steel 09Cr16Ni4Nb, K_σ=1) and by 80 % (Steel 13Cr15Ni4NMo3, K_σ=4). The comparison is made for $N = 2 \bullet 10^6$ cycles. Regarding the maintenance of critical elements, this allows to extend the repair interval by 3–10 times.

Also, the loss of sensitivity to cycle asymmetry for high-strength steels can be explained from the standpoint of a phenomenological approach. By their profession (design engineers and maintenance of industrial equipment), the authors do not study the nature of fatigue failure, but only monitor its manifestations, developing models of equipment behavior under operating conditions. Therefore, in this aspect, the proposed approach looks logical. It is known that the particularly high strength achieved by HSS steels (above 800 MPa) is usually associated with a significant increase in their sensitivity to cyclic loading and, ultimately, with limitations in their crack resistance and fatigue resistance (Junior et al., 2025). The relative endurance limit at a symmetric cycle σ_{-1r}, which is determined for smooth samples, actually acts as an indicator of the sensitivity of the material to cyclic loading. In this case, σ_{-1r}=0.18 (Steel 13Cr15Ni4NMo3), σ_{-1r}=0.33 (Steel 09Cr16Ni4Nb) were obtained. These are rather low values. Typically, high-strength structural steels have σ_{-1r}=0.4–0.5 (Anon, 1990). Despite the fact that the studied steels are high-strength, they have a relatively low fatigue resistance. An intensive decrease in fatigue resistance occurs for the material itself. Therefore, operational factors, for example, cycle asymmetry, can no longer significantly affect the fatigue limit, which looks like a loss of sensitivity to this factor.Table 6.

5. Conclusions

(1). The loss of sensitivity of high-strength steels 13Cr15Ni4NMo3 and 09Cr16Ni4Nb to the medium stress factor was revealed, as evidenced by the form of Smith diagrams (LAD). This phenomenon is explained by the presence of the lowest possible endurance limit σ_{ath} in materials, which forms the limit 2 of the existence of LAD. In turn, the presence of such a limit is due to the behavior of critical ΔK_{fc} and threshold ΔK_{th} SIF with an increase in the stress ratio R. The function $\Delta K_{fc}(R)$ was experimentally obtained, which also has an exponential form. Similar exponential form was also obtained for Smith charts. The use of obtained models compared to traditional ones when servicing critical members makes it possible to increase their repair interval from 3 to 10 times.

(2). A model of the equation of durability based on the concept of merging fracture mechanics and fatigue methodology is proposed. Its application in practice is a priority and requires the assignment of only one parameter in the form of an indicator of slope *S-N* curve. Margin of error when using this model does not exceed 10 % compared to experimental results.

(3). The authors associate further studies of the influence of the cycle asymmetry factor with finding out the reasons for the absence of a threshold fatigue limit σ_{ath} in a certain group of metals. After all, considerations about the presence of limit 2 of the existence of the LAD seem to be valid for most materials.

CRediT authorship contribution statement

S. Belodedenko: Writing – review & editing, Supervision, Methodology, Conceptualization. **O. Hrechanyi:** Writing – review & editing, Visualization, Methodology, Formal analysis. **M. Scherbinin:** Writing – review & editing, Writing – original draft, Resources.

Declaration of competing interest

The authors declare that they have no known competing financial interests or personal relationships that could have appeared to influence the work reported in this paper.

Data availability

Data will be made available on request.

References

Abasolo, M., Pallares-Santasmartas, L., Eizmendi, M., 2024. A new critical plane multiaxial fatigue criterion with an exponent to account for high mean stress effect. Metals 14 (9), 964. https://doi.org/10.3390/met14090964.

Bai, X., Wang, X., Chen, H., Xuan, F., Jia, G., 2025. Failure mechanisms transition of hydrogenation reactor: from creep-fatigue to creep-ratcheting. Int. J. Press. Vessels Pip., 105634 https://doi.org/10.1016/j.ijpvp.2025.105634.

Belodedenko, S., Bilichenko, G., Rassokhin, D., 2025. Engineering safety in the aspect of the safety and security civilization. Emerg. Manag. Sci. Technol. 5 (1). https://doi.org/10.48130/emst-0025-0001, 0.

Belodedenko, S., Hanush, V., Baglay, A., Hrechanyi, O., 2020. Fatigue resistance models of structural for risk based inspection. Civ. Eng. J. 6 (2), 375–383. https://doi.org/10.28991/cej-2020-03091477.

Belodedenko, S., Hrechanyi, O., Hanush, V., Izhevskyi, Y., 2024. Experimental and analytical ways of finding the function of the maximum accumulated damage under operating modes with overloads. Adv. Ind. Manuf. Eng., 100137 https://doi.org/10.1016/j.aime.2024.100137.

Belodedenko, S., Hrechanyi, O., Vasilchenko, T., Baiul, K., Hrechana, A., 2023. Development of a methodology for mechanical testing of steel samples for predicting the durability of vehicle wheel rims. Results. Eng. 18, 101117. https://doi.org/10.1016/j.rineng.2023.101117.

Carpinteri, A., 1992. Elliptical-arc surface cracks in round bars. Fatigue Fract. Eng. Mater. Struct. 15 (11), 1141–1153. https://doi.org/10.1111/j.1460-2695.1992.tb00039.x.

Gomes, V.M.G., de Figueiredo, M.A.V., Correia, J.A.F.O., de Jesus, A.M.P., 2025. Predicting Fatigue Life of 51CrV4 steel parabolic leaf springs manufactured by hot-forming and heat treatment: a mean stress probabilistic modeling approach. Met 15 (3), 315. https://doi.org/10.3390/met15030315.

Haibach, E., 2006. Fatigue Strength – Methods and Data For Evaluation of Components, 3rd edition. Springer-Verlag, Berlin, Heidelberg (in German).

He, Q., Yam, M.C.H., Ho, H.C., Chung, K.-F., 2025. Microstructure-informed crystal plasticity for HCF initiation life of HSS Q690. Int. J. Mech. Sci., 110981 https://doi.org/10.1016/j.ijmecsci.2025.110981.

Jiao, H., Li, M., Yang, X., 2025a. Experimental study and crystal plasticity simulation of low-cycle fatigue behavior for bake-hardening high-strength steels. Int. J. Fatigue, 109236. https://doi.org/10.1016/j.ijfatigue.2025.109236.

Jiao, J., Du, H., Deng, J., Chen, P., Lu, G., 2025b. Experimental and theoretical investigation of the high-cycle fatigue failure mechanism of M24 high-strength bolts. J. Constr. Steel. Res. 230, 109560. https://doi.org/10.1016/j.jcsr.2025.109560.

Junior, L.A.G., Jiménez, S., Cornejo, A., Gustafsson, D., Olsson, E., Barbu, L.G., 2025. Numerical assessment of the high cycle fatigue behavior of high strength steels affected by shear-cutting operations. Int. J. Fatigue, 109178. https://doi.org/10.1016/j.ijfatigue.2025.109178.

Karolczuk, A., Kurek, A., 2025. Machine learning insight into the mean stress impact on fatigue life of additively manufactured 18Ni300 maraging steel under various multiaxial stress paths. Int. J. Fatigue, 109023. https://doi.org/10.1016/j.ijfatigue.2025.109023.

Krejsa, Martin, Brozovsky, Jirí, Lehner, Petr, Parenica, Premysl, 2025. Stanislav Seitl; Fatigue resistance of structural elements made from high-strength steel. AIP. Conf. Proc. 3315 (1), 120003. https://doi.org/10.1063/5.0286010, 11 September.

Krizhanovsky, V.I., Kasperskaya, V.V., Pogrebnyak, A.D., 2008. Evaluation of limit state of structural steels under asymmetric multicycle loading by tension, compression, bending and torsion. Probl. Prochnosti 5, 81–88 [in Russian].

Kujawski, D., Ellyin, F., 1984. A fatigue crack propagation model. Eng. Fract. Mech. 20 (5–6), 695–704. https://doi.org/10.1016/0013-7944(84)90079-1.

Li, B., Liu, P., Cheng, Y., Wang, X., Ren, X., 2025. Probabilistic modeling of fatigue life prediction of notched specimens combining highly stressed volume and theory of critical distance approach. Met 15 (12), 1300. https://doi.org/10.3390/met15121300.

Liu, X., Guo, W., Song, X., Dong, Y., Yang, Z., 2024. Experimental study of the fatigue failure behavior of aluminum alloy 2024-T351 under multiaxial loading. Eng. Fail. Anal. 164, 108684. https://doi.org/10.1016/j.engfailanal.2024.108684.

Lukáš, P., Kunz, L., 1981. Influence of notches on high cycle fatigue life. Mater. Sci. Eng. 47 (2), 93–98. https://doi.org/10.1016/0025-5416(81)90213-5.

Lukash, P., Kunz, L., 1983. Model of critical microcracks at the fatigue limit and its consequences for calculations of cyclic strength. Mechanical fatigue of metals. Kyiv: Nauk. Dumka 224–231.

Macek, W., Marciniak, Z., Branco, R., Rozumek, D., Królczyk, G.M., 2021. A fractographic study exploring the fracture surface topography of S355J2 steel after pseudo-random bending-torsion fatigue tests. Measurement 178, 109443. https://doi.org/10.1016/j.measurement.2021.109443.

More, S.S., Vaara, J., Kärkkäinen, K., Väntänen, M., Frondelius, T., Mayer, H., Schönbauer, B.M., 2025. Defect sensitivity of high-strength steel 42CrMo4: the role of crack initiation and non-propagation defining the fatigue limit. Int. J. Fatigue, 109147. https://doi.org/10.1016/j.ijfatigue.2025.109147.

Newman, J.C., 1998. The merging of fatigue and fracture mechanics concepts: a historical perspective. Prog. Aerosp. Sci. 34 (5–6), 347–390. https://doi.org/10.1016/s0376-0421(98)00006-2.

Oding, I.A., 1962. Permissible Stresses in Mechanical Engineering and Cyclic Strength of Metals. Mashgiz Publ., Moscow, p. 260 p (in Russian).

/Ed. by Anon, 1990. In: Panasyuk, V.V. (Ed.), Mechanics of Fracture and Strength of Metals, Mechanics of Fracture and Strength of Metals, 4. Nauk. DUMKA, Kiev, p. 680. /Ed. byp (in Russian).

Rennert, R., Vormwald, M., Esderts, A., 2024. FKM-guideline “analytical strength assessment” – background and current developments. Int. J. Fatigue, 108165. https://doi.org/10.1016/j.ijfatigue.2024.108165.

Shiozawa, K., Kuroda, Y., Nishino, S., 1998. Effect of stress ratio on subsurface fatigue crack initiation behavior of beta-type titanium alloy. Trans. Jpn. Soc. Mech. Eng. A 64 (626), 2528–2535. https://doi.org/10.1299/kikaia.64.2528.

Susmel, L., 2013. On the estimation of the material fatigue properties required to perform the multiaxial fatigue assessment. Fatigue Fract. Eng. Mater. Struct. 36 (7), 565–585. https://doi.org/10.1111/ffe.12035.

Taylor, D., 1999. Geometrical effects in fatigue: a unifying theoretical model. Int. J. Fatigue 21 (5), 413–420. https://doi.org/10.1016/s0142-1123(99)00007-9.

Toribio, J., 2022. Review and synthesis of stress intensity factor (SIF) solutions for elliptical surface cracks in bolts under tension loading: a Tribute to Juan de la Cierva. Procedia Struct. Integr. 37, 1037–1042. https://doi.org/10.1016/j.prostr.2022.02.042.

Toribio, J., González, B., Matos, J.-C., 2022. Review and synthesis of stress intensity factor (SIF) solutions for elliptical surface cracks in round bars under tension loading: a Tribute to Leonardo Torres-Quevedo. Procedia Struct. Integr. 37, 1029–1036. https://doi.org/10.1016/j.prostr.2022.02.041.

Yue, P., Zhou, C., Zhang, J., Zhang, X., Du, X., Liu, P., 2024. A comparative study on combined high and low cycle fatigue life prediction model considering loading interaction. Int. J. Damage Mech. https://doi.org/10.1177/10567895241292747.

Zeng, B., Jin, L., Yang, Y., Wei, X., Zhang, K., 2025. Simulation of ratcheting behavior and prediction of the fatigue life of HRB400 steel based on crystal plasticity analysis. Fatigue Fract. Eng. Mater. Struct. https://doi.org/10.1111/ffe.70050.

Zhao, X., Li, J., Sun, T., Wang, S.-S., Deng, H., Zhu, J.-G., Xia, J., 2025. Research on local cyclic plastic behavior and fatigue life prediction of notched components based on digital image correlation. Theor. Appl. Fract. Mech., 105045 https://doi.org/10.1016/j.tafmec.2025.105045.